

# UC Irvine

## UC Irvine Previously Published Works

### Title

Distribution of two-level system couplings to strain and electric fields in glasses at low temperatures

### Permalink

<https://escholarship.org/uc/item/2qr0j1z5>

### Journal

Physical Review B, 104(13)

### ISSN

2469-9950

### Authors

Carruzzo, Herve M  
Bilmes, Alexander  
Lisenfeld, Jürgen  
[et al.](#)

### Publication Date

2021-10-01


### DOI

10.1103/physrevb.104.134203


Peer reviewed

**Distribution of two-level system couplings to strain and electric fields in glasses at low temperatures**

Herve M. Carruzzo

*Department of Physics and Astronomy, University of California, Irvine, Irvine, California 92697, USA*Alexander Bilmes  and Jürgen Lisenfeld*Physikalisches Institut, Karlsruhe Institute of Technology, 76131 Karlsruhe, Germany*Zheng Yu *Department of Materials Science and Engineering University of Wisconsin-Madison, Madison, Wisconsin 53706, USA*

Bu Wang

*Department of Civil and Environmental Engineering University of Wisconsin-Madison, Madison, Wisconsin 53706, USA*Zhongyi Wan  and J. R. Schmidt*Department of Chemistry University of Wisconsin-Madison, Madison, Wisconsin 53706, USA*Clare C. Yu \**Department of Physics and Astronomy, University of California, Irvine, Irvine, California 92697, USA*

(Received 30 August 2021; accepted 6 October 2021; published 26 October 2021)

The thermal, acoustic, and dielectric properties of glasses below 1 K are dictated by the interaction of two-level systems (TLS) with strain and electric fields. In a previous paper, we proposed a modified TLS model to quantitatively account for the universally small phonon scattering in glasses at low temperatures. A key ingredient of this model was a wide distribution of couplings between TLS and phonons, contrary to the standard model which assumes a single averaged value is sufficient. In this paper, we expand on this view and include couplings to strain as well as electric fields. We then compare our theoretical results to measurements obtained using superconducting qubits. We find that the predictions of the modified TLS model are more consistent with experiments than those of the standard model. For the distribution of couplings between TLS and the strain field, there is a better agreement with experiments if we include a random distribution of local strains. Such a distribution of local strains is consistent with those found from molecular dynamics simulations.

DOI: [10.1103/PhysRevB.104.134203](https://doi.org/10.1103/PhysRevB.104.134203)**I. INTRODUCTION**

Glasses at low temperature exhibit a number of anomalous features compared to crystals. Chief among them are the specific heat which is linear in temperature  $T$  and the thermal conductivity which is quadratic in  $T$ . These anomalies have been successfully described by the model of tunneling two level systems (TLS) [1–4]. This model posits the existence of localized regions, an atom or group of atoms for example, that can tunnel between two nearly equivalent states. These tunneling entities, being embedded in the glass matrix and often carrying an electric dipole moment, interact with electric and elastic fields. However, the standard model, i.e., the model as it was originally proposed, does not quantitatively explain the universal values of phonon scattering below 1 K as reflected in the thermal conductivity (scaled with natural units) [5], internal friction (in the relaxation regime) [6], the change in the sound velocity, and the resonant ultrasonic attenuation [7]. Recently, Carruzzo and Yu proposed a modified TLS model

to quantitatively explain the universally small value of the phonon scattering [8]. Their explanation was based on aspects of the standard TLS model that were either ignored or not fully appreciated. First, the coupling between phonons and TLS implies that the TLS can interact with each other [9]. Second, this coupling produces an exponential renormalization of the tunneling matrix element due to phonon overlap between the two wells (a kind of polaron effect) [10]. Third, phonons actually couple to the difference between elastic dipole moments in the two wells. If the elastic dipole moment in each well has a random orientation, the difference will vary randomly from TLS to TLS, leading to a broad distribution of couplings as opposed to the standard model that assumes a single value of the coupling. One way to differentiate between the standard and the modified model would be to measure the distribution of couplings between TLS and the strain field. However, until recently, the values of these couplings for *individual* TLS have been out of experimental reach. This lack of direct access to these tunneling entities—the very question of exactly what is tunneling is still unclear in most cases—makes it difficult to constrain the model. At least for some of the aspects of these TLS, the situation is changing with the advent of super-

\*Corresponding author: [cyy@uci.edu](mailto:cyy@uci.edu)

conducting qubit and resonator spectroscopy [11,12]. These techniques allow experimental observation of the interaction between an individual TLS and a superconducting quantum circuit, and thus extract TLS-specific information [13]. The purpose of this paper is to differentiate between the standard and modified TLS models using qubit and resonator spectroscopy measurements of the distribution of TLS-field (strain or electric) coupling strengths. In particular, we will answer the question of whether the distribution of these couplings are they peaked around some characteristic value, as assumed in the standard TLS model, or spread out over a broad range.

Let us briefly review the TLS model. A TLS is an atom or group of atoms that can sit more or less equally well in two configurations and tunnel between them. This is described by a double well potential with a barrier separating the two wells. Keeping only the lowest energy state in each well simplifies the Hamiltonian representing a given TLS to the form:

$$H_{\text{TLS}} = \frac{1}{2}(\Delta\sigma^z + \Delta^o\sigma^x), \quad (1)$$

where  $\Delta$  is the asymmetry energy and  $\Delta^o$  is the tunneling matrix element. The values of these parameters are assumed to vary from TLS to TLS according to the probability distribution:

$$P(\Delta, \Delta^o) = \frac{\bar{P}}{\Delta^o} \quad (2)$$

with  $0 < \Delta < \Delta_{\text{max}}$  and  $\Delta_{\text{min}}^o < \Delta^o < \Delta_{\text{max}}^o$ .  $\bar{P}$  is the constant density of states of tunneling entities.

TLS primarily interact with electric and elastic fields. Quite generally, the coupling between a TLS and an electric field  $\vec{E}$  is given by

$$D_a \equiv \frac{\delta H_{\text{TLS}}}{\delta E_a}, \quad (3)$$

where  $E_a$  is the component of the electric field along axis  $a = x, y, z$ . This defines the electric dipole moment  $D_a$ . Likewise, the coupling to an elastic strain  $\epsilon_{ab}$  is given by

$$\mathcal{D}_{ab} \equiv \frac{\delta H_{\text{TLS}}}{\delta \epsilon_{ab}}, \quad (4)$$

where  $\mathcal{D}_{ab}$  is the elastic dipole moment, a symmetric tensor. The Hamiltonian describing the interaction of a TLS with these fields can therefore be written

$$H_{\text{int}} = \vec{D} \cdot \vec{E}\sigma_z + \mathcal{D}_{ab}\epsilon_{ab}\sigma_z. \quad (5)$$

In the above expression, terms proportional to  $\sigma^x$  are assumed to be much smaller and therefore neglected. It will be useful for the rest of this discussion to separate explicitly the norm of the dipole moments from their vectorial or tensorial nature and write the interaction Hamiltonian in the form:

$$H_{\text{int}} = d\hat{D} \cdot \vec{E}\sigma_z + \gamma\hat{\mathcal{D}}_{ab}\epsilon_{ab}\sigma_z, \quad (6)$$

where  $d$  is the norm of  $\vec{D}$ ,  $\hat{D}$  is the unit vector along  $\vec{D}$ ,  $\gamma = \|\mathcal{D}\|_F$  and  $\hat{\mathcal{D}}_{ab} = \mathcal{D}_{ab}/\gamma$ , where  $\|\cdot\|_F$  is the Frobenius norm. One can imagine that the orientation of the electric dipole  $\hat{D}$  varies randomly from TLS to TLS. Given that the eigenvalues of a symmetric matrix like  $\mathcal{D}$  defines an ellipsoid, its ‘‘orientation’’ may also be considered to vary randomly from TLS to TLS even if its eigenvalues do not change. In the standard TLS model,  $d$  and  $\gamma$  are considered constants.

As mentioned above, the modified TLS model predicts a wide range of values for these parameters [8] (see also Ref. [14]). Can the newly developed qubit spectroscopy methods help decide which view is more appropriate? This is the main topic of this work.

The rest of this paper is organized as follows. First the derivation of Eq. (6) will be done more carefully, mirroring closely the discussion in Ref. [8]. It will become apparent that the assumption of a single value for the strength of the electric dipole moment or for that of the elastic dipole moment is unlikely to be correct. Rather, in this modified TLS model, a distribution of values is to be expected. The following section concentrates on calculating likely distributions for these couplings on the basis of that model. The dielectric and elastic cases are treated separately due to their different tensorial natures. This is then followed by a comparison of the theoretical results (including the standard TLS model) to a series of experiments (Refs. [12,15]) that probe the coupling of individual TLS to static electric and strain fields.

## II. TLS - FIELDS INTERACTION REVISITED

In the introduction, the dipole moments—electric or elastic—were defined formally. Practically, one has to consider the operator for the electric or elastic dipole moment as expressed in the double well basis of the TLS model. With  $\mathbf{D}$  denoting either moment, the projection of this operator on the right and left basis states  $|\psi_{R,L}\rangle$  of the two well potential is

$$\begin{aligned} \mathbf{D} &= \begin{bmatrix} D^{LL} & D^{LR} \\ D^{RL} & D^{RR} \end{bmatrix} \\ &= \frac{1}{2}(D^{LL} + D^{RR})\mathbf{I} + \frac{1}{2}(D^{LL} - D^{RR})\sigma^z + D^{LR}\sigma^x, \quad (7) \end{aligned}$$

where  $D^{AB} \equiv \langle \psi_A | \mathbf{D} | \psi_B \rangle$ .  $\mathbf{I}$  is the identity matrix and thus this term can be dropped.  $D^{LR} = D^{RL}$  depends on the overlap between the right and left wells and hence is taken to be negligible. As a result, only the  $\sigma^z$  term remains. *The key is that the  $\sigma^z$  term is half the difference of the dipole moment  $D$  in the right and left wells:*

$$\mathbf{D} = \frac{1}{2}(D^{LL} - D^{RR})\sigma^z. \quad (8)$$

The standard TLS model makes the assumption that this difference is constant and the same for all TLS. Given the substantial local variations in amorphous materials, this does not seem like a reasonable assumption. The opposite viewpoint is taken in this work, namely, that the dipole moments in the right and left well are uncorrelated, at least in some aspects. This will be made more specific in the subsequent discussion of the dielectric and elastic cases. The important point is that the net dipole describing the coupling to the field is a difference of two uncorrelated dipoles and therefore will have to be characterized by a distribution instead of a single value.

### A. Dielectric case

The dielectric case is simpler and instructive. An electric dipole moment is characterized by its orientation and magnitude. The difference of two such dipoles is itself specified by an orientation and magnitude. The task is therefore to

calculate the distributions of the magnitude and orientation of (half) the difference between the electric dipoles in each well. Without loss of generality, the right well dipole can be chosen to be along the  $z$  axis:  $\vec{d}_R = d_o \hat{z}$ . The left well dipole is then  $\vec{d}_L = \vec{d}_o \hat{n}$  where  $\hat{n}$  is a unit vector pointing in an arbitrary direction. While  $d_o$  and  $\vec{d}_o$  could vary between 0 and some maximal value, choosing  $d_o = \vec{d}_o = \text{constant}$  simplifies the algebra. To leading order, allowing  $d_o$  and  $\vec{d}_o$  to be distributed uniformly between 0 and some maximal value, does not materially change the result. The quantity of interest is then  $d^2 = |\hat{z} - \hat{n}|^2 d_o^2 / 4$  where  $d_o$  is a fixed quantity of the order of a Debye. Assuming that  $\hat{n}$  is uniformly distributed on the unit sphere with angles  $\theta$  and  $\phi$ ,  $d^2$  has the following probability distribution:

$$P(d^2) = \frac{1}{4\pi} \int_0^{2\pi} d\phi \int_0^\pi d\theta \sin(\theta) \delta(d^2 - d_o^2(1 - \cos(\theta))/2) \\ = \frac{1}{d_o^2} \quad 0 < d^2 < d_o^2 \quad (9)$$

or, equivalently,

$$P(d) = \frac{2d}{d_o^2}, \quad 0 < d < d_o. \quad (10)$$

While the distribution is “peaked” at the largest value of the dipole moment, keeping only a single value for  $d$ , such as  $d_o$  or the average value of  $d$ , is not a good approximation. How one can experimentally determine the distribution of coupling strengths will be taken up in Sec. III, while the next section is devoted to the elastic case.

### B. Elastic case

The elastic case immediately presents a problem. Unlike the single invariant in the vector case, the (symmetric) elastic dipole tensor  $\mathbf{D}$  has three invariants:  $\text{Tr}(\mathbf{D})$ ,  $\text{Tr}(\mathbf{D}^2)$ , and  $\text{Det}(\mathbf{D})$ . There is, therefore, a question as to how these invariants enter the picture. When calculating quantities such as ultrasonic absorption or TLS relaxation times, it is typically sufficient to use first order perturbation theory. The quantities depending on  $\mathbf{D}$  then always enter the equations as

$$\langle (\text{Tr}[\mathbf{D}\epsilon^\alpha])^2 \rangle, \quad (11)$$

where  $\epsilon^\alpha$  stands for the elastic tensor  $\epsilon_{ij}^\alpha = \frac{1}{2}(\hat{e}_i^\alpha \hat{k}_j + \hat{e}_j^\alpha \hat{k}_i)$ ,  $i, j = x, y, z$ ,  $\hat{e}^\alpha$  is a polarization vector for the  $\alpha = l, t$  polarization and  $\hat{k}$  is a phonon unit wave vector. The angular

brackets denote the average over dipole orientations or equivalently, average over phonons directions  $\hat{k}$  when considering a single TLS. Equation (11) is the square of the TLS-phonon coupling usually denoted by  $\gamma_\alpha^2$  in the TLS literature. In the case of longitudinal phonons, Eq. (11) gives

$$\gamma_l^2 = \langle (\text{Tr}[\mathbf{D}\epsilon^l])^2 \rangle = \frac{1}{15}(2\text{Tr}(\mathbf{D}^2) + (\text{Tr}(\mathbf{D}))^2), \quad (12)$$

while the result for the transverse case is

$$\gamma_t^2 = \langle (\text{Tr}[\mathbf{D}\epsilon^t])^2 \rangle = \frac{1}{30}(3\text{Tr}(\mathbf{D}^2) - (\text{Tr}(\mathbf{D}))^2). \quad (13)$$

A few conclusions can be drawn from these very general relations. The first is that, even when TLS-phonon interactions are handled at the lowest order in perturbation theory as described above, it is not possible to simply summarize the elastic dipole strength by a single number. The second is that the longitudinal coupling is always larger than the transverse one. The third is that an isotropic dipole tensor only couples to longitudinal phonons. Note also that a volume conserving tensor [i.e., with  $\text{Tr}(\mathbf{D}) = 0$ ] implies a ratio  $\gamma^l/\gamma^t = 2/\sqrt{3} \sim 1.15$  which is significantly smaller than what is observed experimentally ( $\sim\sqrt{3}$ , see Ref. [7]). Thus far nothing has been said about the form of  $\mathbf{D}$ . The most general form of such a symmetric tensor can be expressed as  $D_{ij} = a + b\hat{n}_i\hat{n}_j + c\hat{m}_i\hat{m}_j$ , where  $\hat{n}$  and  $\hat{m}$  are arbitrary unit vectors and  $a, b, c$  are real numbers. Interestingly, the simplest such dipole,  $a = 0, c = 0$ , results in  $\gamma^l/\gamma^t = \sqrt{3}$ , which is very close to the ratio observed experimentally [7]. To see this, notice that with a single unit vector  $\hat{n}$ , the dipole tensor has one diagonal element equal to  $b$  and zero for all other matrix elements. In that case,  $\text{Tr}(\mathbf{D}^2) = (\text{Tr}(\mathbf{D}))^2$  from which the result follows.

As in the dielectric case, the relevant quantity is the difference in dipole moment between the two wells of the TLS. Using the same assumption, namely, that the dipoles are identical yet “oriented” differently but uniformly with respect to each other, the quantity of interest is:  $\Delta\mathbf{D} = \frac{1}{2}(\mathbf{D}_o - \mathbf{R}^T \mathbf{D}_o \mathbf{R})$ , where  $\mathbf{R}$  denotes a rotation (uniform rotation around a unit vector uniformly distributed over the unit sphere).  $\mathbf{D}_o$  is the typical dipole moment in one well, taken to be the same for all TLS. The most general case with three distinct eigenvalues for  $\mathbf{D}_o$  is not amenable to an analytic solution for  $\Delta\mathbf{D}$ . The case where there is only one nonzero eigenvalue,  $\lambda$ , has an analytic solution (this corresponds to building the dipole moment out of a single unit vector). Another solvable case is when the dipole moment has only two distinct values  $\lambda_1$  and  $\lambda_2$ . The first case is presented below. The rotation matrix  $\mathbf{R}$  is given by

$$\begin{bmatrix} \cos(\psi)\cos(\phi)\cos(\theta) - \sin(\psi)\sin(\phi) & -\sin(\psi)\cos(\phi) - \cos(\psi)\sin(\phi)\cos(\theta) & \cos(\psi)\sin(\theta) \\ \sin(\psi)\cos(\phi)\cos(\theta) + \cos(\psi)\sin(\phi) & \cos(\psi)\cos(\phi) - \sin(\psi)\sin(\phi)\cos(\theta) & \sin(\psi)\sin(\theta) \\ -\cos(\phi)\sin(\theta) & \sin(\phi)\sin(\theta) & \cos(\theta) \end{bmatrix}, \quad (14)$$

where the Euler angles  $\psi$  and  $\phi$  range from 0 to  $2\pi$  and  $\theta$  ranges from 0 to  $\pi$ . (Convention:  $\mathbf{R}$  is obtained by a  $\psi$  rotation around the current  $z$  axis followed by a  $\theta$  rotation around the current  $y$  axis, followed by a  $\phi$  rotation around the current  $z$  axis.)

A straightforward if tedious calculation gives for  $\Delta\mathbf{D}$  in its diagonal basis

$$\Delta\mathbf{D} = \lambda \sin(\theta) \begin{bmatrix} -1 & 0 & 0 \\ 0 & 1 & 0 \\ 0 & 0 & 0 \end{bmatrix}, \quad (15)$$

where  $0 \leq \theta \leq \pi$ . (The second case with two eigenvalues  $\lambda_1$  and  $\lambda_2$  gives the same result with  $\lambda$  replaced by  $\lambda_1 - \lambda_2$ .) The trace of  $\Delta D$  is zero and, therefore, from Eqs. (12) and (13),

$$\gamma_l = \frac{2\lambda}{\sqrt{15}} \sin(\theta) \equiv \gamma_{\max,l} \sin(\theta) \quad (16)$$

and

$$\gamma_t = \frac{\lambda}{\sqrt{5}} \sin(\theta) \equiv \gamma_{\max,t} \sin(\theta), \quad (17)$$

where  $\gamma_{\max,l} = 2\lambda/\sqrt{15}$  and  $\gamma_{\max,t} = \lambda/\sqrt{5}$ . Using the fact that  $P(\gamma_p) = P(-\gamma_p)$ , the probability of obtaining a given  $|\gamma_p|$  ( $p = l, t$ ) is then

$$\begin{aligned} P(\gamma_p) &= \int_0^{\pi/2} d\theta \sin(\theta) \delta(\gamma_p - \gamma_{\max,p} \sin(\theta)) \\ &= \frac{\gamma_p}{\gamma_{\max,p}^2 \sqrt{1 - \gamma_p^2/\gamma_{\max,p}^2}}, \quad 0 < \gamma_p < \gamma_{\max,p}. \end{aligned} \quad (18)$$

As argued in Ref. [8], this can reasonably well be approximated by  $P(\gamma_p) \sim \gamma_p/\gamma_{\max,p}^2$ . The problem here is that by construction, the trace of the dipole moment difference is zero which means that the ratio  $\gamma_l/\gamma_t$  is smaller than experiments suggest [7]. This can be remedied at the expense of additional assumptions as to the way the dipoles in each well differ. Given the lack of a detailed microscopic model, there is little point in doing so. The main element to emphasize is that a distribution of coupling constants  $\gamma_{l,t}$  should be expected.

It is worth noting that Parshin *et al.* [14] also obtained a distribution of TLS-phonon couplings in their approach to TLS formation based on the instability of quasi-elastic vibrations.

### III. EXPERIMENTAL MEASUREMENTS OF THE TLS-FIELD COUPLINGS

TLS with electric dipole moments are a major source of decoherence in superconducting qubits because a TLS in resonance with the qubit can split the qubit energy levels [16]. While this is a major headache in the field of quantum computing [11], this coupling allows us to observe individual TLS and their coupling to AC electric fields. In addition, the dependence of the TLS energy splitting on static electric fields and strain fields can also be extracted [15,17].

Consider an amorphous material in close proximity to a qubit at a temperature  $T$  much less than the qubit excitation energy  $\hbar\omega_q$  (the experimental setup is described in Ref. [17]). In general, this material will contain many TLS with electric dipole moments. The qubit is prepared in its excited or  $|1\rangle$  state. If there is a TLS with an energy splitting  $E = \hbar\omega_q$  where  $\omega_q$  is the qubit's frequency, energy will be exchanged between the qubit and the TLS. If the relaxation time  $T_{1,\text{TLS}}$  of the TLS is short enough ( $T_{1,\text{TLS}} \ll T_{1,\text{qubit}}$ ) which is usually the case, the loss of the qubit's excitation can be detected. This is done by measuring the probability  $P$  that the qubit is in its excited state after a time  $t$ . If  $T_{1,\text{TLS}}$  is sufficiently short,  $P(t)$  will decay exponentially. For intermediate values of  $T_{1,\text{TLS}}$ , oscillation may be observed in the exponential decay, reflecting energy moving back and forth between the qubit and the TLS. From the decay of  $P(t)$  the relaxation time  $T_{1,\text{qubit}}$  can be

extracted. If  $T_{1,\text{qubit}}$  is significantly reduced and the qubit is in resonance with a TLS, its energy can thus be measured. With a tunable qubit, the frequency  $\omega_q$  can be changed continuously between a minimum and maximum value. During a frequency sweep, different TLS will come into resonance with the qubit. Now consider what happens upon the application of a static field  $F$  with coupling  $p$  to the TLS. ( $F$  can be either an electric field or a strain field.) As a function of the static external field, the TLS energy will be

$$\varepsilon = \sqrt{\Delta_o^2 + (\Delta + 2pF)^2}, \quad (19)$$

where  $\Delta$  is the asymmetry energy and  $\Delta_o$  is the tunneling energy of the TLS. Thus if a frequency scan  $\omega_{q,\min} < \omega_q < \omega_{q,\max}$  is performed for each value of the external field, the point of maximal qubit energy loss, when  $\hbar\omega_q$  equals the TLS energy splitting, will show up as a curve tracing Eq. (19) on a 3D density plot of  $T_{1,\text{qubit}}$  with  $F$  on the horizontal axis and  $\omega_q$  on the vertical axis. A good example is shown in Fig. 1 (but see also Figs. 2(c) and 2(d) of Ref. [17]). A fit of such a trace to Eq. (19) allows the extraction of  $\Delta_o$  and  $p$ , at least if  $\Delta_o/\hbar$  lies between the minimum and maximum frequency of the qubit.

An alternative to using qubits as the detector is to use an LC circuit, as described in Ref. [15]. The principle is similar but instead of measuring the state of a qubit, the loss in the LC resonator at its natural frequency  $\omega_{\text{LC}}$  is measured. When a TLS is at resonance with the LC circuit, the loss in the latter will be large. A 3D plot of the LC circuit loss with  $F$  on the horizontal axis and  $\omega_{\text{LC}}$  on the vertical axis will again show traces where the loss is large following Eq. (19). An example is shown in Fig. 2 of Ref. [15].

It is important to note that regardless of whether the static field  $F$  is elastic or electric, the coupling of the TLS to the qubit or resonator is via photons with frequency  $\omega_q$ . If  $d_{\parallel}$  denotes the component of the electric dipole moment parallel to the direction of the AC electric field of the qubit, then the TLS coupling strength is  $d_{\parallel}E_{\text{AC}}\Delta^o/\varepsilon$ . Thus TLS with very small values of  $d_{\parallel}\Delta^o/\varepsilon$  will essentially be invisible. In the standard TLS model,  $\varepsilon$ ,  $\Delta^o$ , the electric dipole moment and the elastic dipole moment are all uncorrelated quantities. Therefore the TLS-qubit coupling has no impact on the distribution of couplings that are observed, just an overall reduction of the total number of TLS that can be observed. The modified TLS model differs in this respect since  $\Delta^o$  and the magnitude of the elastic dipole moment are correlated in that model. In fact, the two quantities are related by

$$\Delta^o = \Delta_{\max}^o e^{-(\gamma/\gamma_o)^2}, \quad (20)$$

where  $\gamma$  is the magnitude of the elastic dipole moment averaged over longitudinal and transverse polarizations and  $\gamma_o$  is a constant depending on material parameters.  $\gamma_o$  is  $\sim 0.25$  eV in the case of  $\text{SiO}_2$ . This relation between  $\Delta^o$  and  $\gamma$  stems from the phonon-TLS coupling which produces an exponential renormalization of the tunneling matrix element due to phonon overlap between the two wells of the TLS (a kind of polaron effect) [8]. Note that the distribution of elastic couplings given by Eq. (18) ensures the distribution Eq. (2) is satisfied up to logarithmic corrections. As a result, TLS with large elastic dipole moments will have a small tunneling

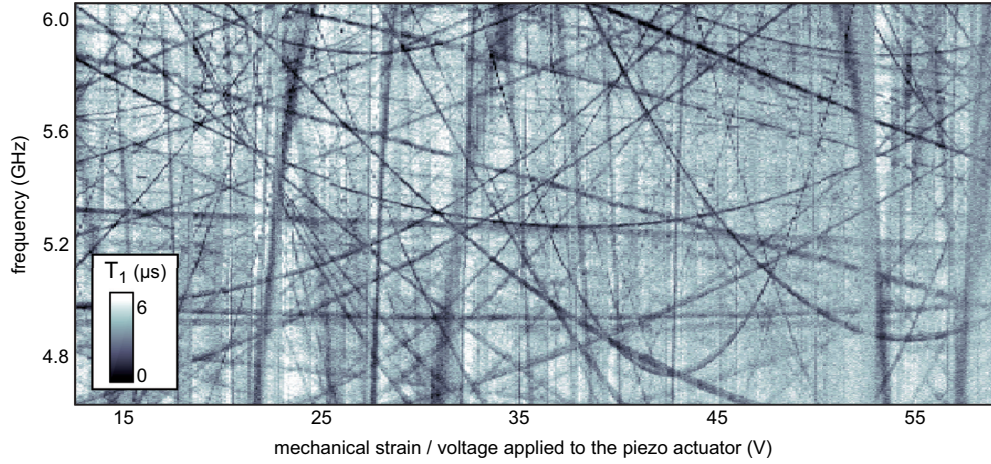


FIG. 1. Energy relaxation time  $T_1$  (gray scale) of a superconducting transmon qubit as a function of the qubit resonance frequency and the applied mechanical strain. Dark hyperbolic traces indicate the resonances of TLS defects which absorb energy from the qubit.

parameter  $\Delta^o$  and thus a reduced coupling to the qubit. This has the effect of selectively suppressing high elastic dipole TLS in the observed distribution of elastic dipoles (see Sec. III B). There is no corresponding effect for electric dipole measurements as electric and elastic dipole moments are assumed to be uncorrelated.

#### A. Dielectric case

Typical experimental setups are described in Refs. [15,17]. A static electric field is applied to the amorphous material in a parallel plate capacitor configuration. A TLS is characterized by its asymmetry energy  $\Delta$ , its tunneling energy  $\Delta_o$  and, in the dielectric case considered here, and an electric dipole moment  $\mathbf{d}$ . The TLS coupling to phonons via the TLS elastic dipole moment is also present and primarily responsible for the TLS relaxation time. As long as TLS relax sufficiently fast on the timescale of the measurement frequencies (GHz range), this coupling is not explicitly needed for the present calculation. The TLS energy splitting  $\varepsilon$  as a function of the applied static electric field  $\mathbf{E}$  is given by

$$\varepsilon = \sqrt{\Delta_o^2 + (\Delta + 2d_z E)^2}, \quad (21)$$

where  $d_z = d \cos(\theta)$  is the projection of the dipole moment along the  $\mathbf{E}$  field taken to be along the  $z$  axis.  $E$  ranges from  $-E_m$  to  $E_m$  with  $E_m \sim 100$  kV/m. The TLS model assumes that the probability of finding a TLS with values  $\Delta$  and  $\Delta_o$  is given by  $P(\Delta, \Delta_o) = \bar{P}/\Delta_o$  with  $-\Delta^{\max} < \Delta < \Delta^{\max}$  and  $\Delta_o^{\min} < \Delta_o < \Delta_o^{\max}$ ;  $\bar{P}$  ensures that the distribution is properly normalized to 1. With the additional assumption that the electric dipole moment is independent of  $\Delta$  and  $\Delta_o$ , the probability density  $P_O(d_z)$  of observing a TLS with dipole moment  $d_z$  satisfies approximately:

$$P_O(d_z) \sim P(d_z) \int_{\hbar\omega_{q,\min}}^{\hbar\omega_{q,\max}} d\varepsilon \int_{-2d_z E_m}^{2d_z E_m} dy \int_{-\Delta^{\max}}^{\Delta^{\max}} d\Delta \int_{\Delta_o^{\min}}^{\Delta_o^{\max}} d\Delta_o \times \frac{d\Delta_o}{\Delta_o} \delta(\varepsilon - \sqrt{\Delta_o^2 + (\Delta + y)^2}), \quad (22)$$

where  $P(d_z)$  is the true probability that a given TLS has electric dipole moment  $d_z$  and  $y = 2d_z E$ . Provided that  $\Delta^{\max} \gg$

$2|d_z E|$  and  $\Delta^{\max} > \hbar\omega_q$ ,  $\Delta$  can simply be shifted by  $y$ . Then the integral over  $y$  simply yields a factor  $4d_z E_m$ . The integral over  $\Delta_o$  and the shifted  $\Delta$  gives a factor independent of  $\varepsilon$ , up to logarithmic accuracy. The last remaining integral, over  $\varepsilon$ , is thus a factor proportional to  $(\hbar\omega_{q,\max} - \hbar\omega_{q,\min})$ . The observed distribution of  $d_z$  is therefore related to the actual distribution by

$$P_O(d_z) = A P(d_z) d_z, \quad (23)$$

where  $A$  is a normalization constant. Another way to understand Eq. (23) is to consider the rectangle defined by the range of values  $\hbar\omega_{q,\min} : \hbar\omega_{q,\max}$  along the  $y$  axis and  $-d_z E : d_z E$  for a given  $d_z$  along the  $x$  axis of the rectangle. Since the number of TLS per unit energy is (nearly) constant, the density of TLS in that rectangle is also constant. Therefore the number of TLS observed will be proportional to the area of the rectangle times the probability of having a given  $d_z$ , which immediately yields Eq. (23). The prediction for the distribution of  $P(d_z)$  in any model must then be adjusted using Eq. (23) when comparing the result with experiments.

Figure 2 shows the distribution  $P_O(d_z)$  obtained from Fig. 3 of Ref. [15]. There are a total of 60 measurements. The data

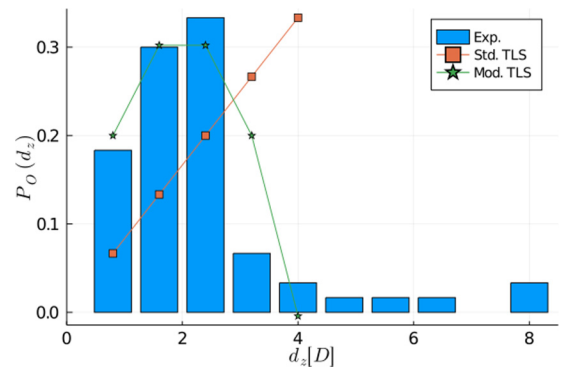


FIG. 2. Raw distribution of  $d_z$  obtained from Fig. 3 of Ref. [15] (Exp.). The squares are the prediction of the standard TLS model with  $d_o = 4$  (Std. TLS). The stars markers are the prediction of the modified TLS model, also with  $d_o = 4$  (Mod. TLS).

appears distinctly different below and above  $d_z \sim 4$  Debye. The authors of that paper have concluded that two types of TLS with distinct dipole moments exist. The same assumption is made here. Given the very small number of data points with  $d_z > 4$ , the two regimes can be qualitatively discussed separately. It is instructive to first consider the prediction of the standard TLS model which posits that  $|\mathbf{d}| = d_o$  with a uniform orientation distribution on the unit sphere. This implies a flat distribution  $P(d_z) = 1/(2d_o)$ ,  $-d_o < d_z < d_o$ . Because of the symmetry  $z \rightarrow -z$ , the experimental data is “folded” to the positive values, so the distribution needed is  $P(|d_z|) = 1/d_o$ . The corresponding distribution for the observed values  $P_O(d_z)$  is obtained by using Eq. (23). The result for the regime  $d_z < 4$  is shown in Fig. 2 by the straight line with square markers, using  $d_o = 4$ . The precise value of  $d_o$  is not important at this qualitative level. Even though the total number of data points is quite small, this set of data clearly does not support the standard TLS model.

The distribution of dipole norms based on the difference between the moment in each well,  $P(d)$ , (modified TLS model) was given by Eq. (10). The projection along the  $z$  direction is

$$P(d_z) = \frac{1}{2} \int_0^\pi d\theta \sin(\theta) \frac{2}{d_o^2} \int_0^{d_o} \delta(d_z - d \cos(\theta)) P(d) dd, \quad (24)$$

which, again folding negative values onto the positive ones, gives

$$P(d_z) = \frac{2}{d_o^2} (d_o - d_z), \quad 0 < d_z < d_o. \quad (25)$$

Again the corresponding observed distribution is obtained from this result using Eq. (23). The result for the region  $d_z < 4$  is shown in Fig. 2 by the star markers, using  $d_o = 4$  as before. At this qualitative level, the general form matches the data better than the standard TLS model.

What can explain the values observed in the range  $d_z > 4$ ? It seems unlikely that a localized moment would be of such a large magnitude. However a group of TLS acting coherently could possibly have a significantly larger effective moment. Consider, for instance, a pair of TLS in relatively close proximity, with equal energy splittings. These two TLS will interact with each other statically via the strain field and via resonant phonon exchange, since the energy splittings are the same. The Hamiltonian of such a system is approximately given by

$$H = \frac{\varepsilon}{2} (\sigma_1^z + \sigma_2^z) - J \sigma_1^z \sigma_2^z + K \sigma_1^x \sigma_2^x, \quad (26)$$

where  $\varepsilon = \sqrt{\Delta_o^2 + (\Delta + 2d_z E)^2}$  is the energy splitting of TLS “1” and “2,”  $J > 0$  and  $K$  are TLS-TLS coupling constants such that  $J \gg |K|$ . The  $z$  component of the electric dipole moment of each TLS,  $d_z$ , is furthermore assumed to be the same (or else the static electric field  $E$  would eliminate the resonant  $\sigma_1^x \sigma_2^x$  term). The two lowest energy eigenstates are found to be a mixture of the  $|11\rangle$  and  $|1-1\rangle$  states with energies  $-J \pm \sqrt{K^2 + \varepsilon^2}$ . The other two eigenstates are higher in energy,  $J \pm K$ , and mix the  $|1-1\rangle$  and  $|11\rangle$  states. The energy difference between the two lowest eigenstates is then  $\sqrt{4K^2 + 4\Delta_o^2 + (2\Delta + 4d_z E)^2}$ . The measured value of

the dipole moment would then be  $2d_z$ . Its maximal value is  $2d_o = 8$  Debye when  $\vec{d} \parallel \vec{E}$ . For these pairs of TLS, the predicted distribution of their dipole moment is identical to the single TLS case (as shown in Fig. 2) with the replacement  $d_o \rightarrow 2d_o$ , albeit with a much lower overall probability of occurrence. There are not enough data points in the range  $4 < d_z < 8$  to draw any conclusion as to the actual distribution of dipole strengths for these pairs. Nevertheless this simple calculation provides a possible explanation for the large dipole values observed while being consistent with a distribution of dipole strengths.

## B. Elastic case

This section mirrors Sec. III A but for the case of a static elastic field. As noted earlier, the present case is more involved. The standard TLS model and the modified TLS model will be used to predict the distribution of the projection of the TLS-phonon coupling along the direction of the externally applied strain field and then compared to the measurements.

The reader is referred to the work of Grabovskij *et al.* for a detailed description of the experimental setup [12]. In a nutshell, the measuring qubit is deposited on a silicon (or sapphire) substrate. This substrate is held fixed at the right and left edges. A piezo controlled rod below the center and perpendicular to it can impart a force to the substrate, bending it slightly. The resulting shear stress is proportional to the vertical displacement of the rod and thus to the voltage  $V_p$  applied to the piezo. This stress will alter the asymmetry energy of TLS near the qubit according to Eq. (19). The term  $2\gamma F$  in that equation now takes the form  $\gamma_z \alpha V_p$ , where  $\gamma_z$  is the magnitude of the projection of the elastic dipole moment along the direction of the applied field and  $\alpha V_p$  is the strain field. Grabovskij *et al.* estimate the coefficient  $\alpha$  to be  $\alpha = 10^{-6}$  per volt as an order of magnitude. Grabovskij *et al.* do not directly measure  $\gamma_z$ , but rather  $\gamma_z \alpha$  in GHz/V and that is the quantity that will be calculated to allow for a direct comparison with experiment.

The first step is to compute the distribution of  $\gamma_z$ . The dipole moment coupling to shear strains, in the basis where the dipole moment is diagonal, can be taken to be of the form:

$$\Delta \mathbf{D} = \gamma_i \begin{bmatrix} -1 & 0 & 0 \\ 0 & 1 & 0 \\ 0 & 0 & 0 \end{bmatrix}, \quad (27)$$

where the distribution for  $\gamma_i$  is given by Eq. (18) for the modified TLS model. For the standard model, it is simply a constant. Since the dipole moment is oriented randomly with respect to the strain field, its expression will be given by Eq. (27) but rotated by an arbitrary rotation  $R$ . This rotated dipole is given by  $R \Delta \mathbf{D} R^{-1}$ , where  $R$  is the matrix representing the arbitrary rotation. This matrix is given by Eq. (14). The next step is to compute  $\gamma_z \equiv \gamma_i \tilde{\epsilon}_{ij} (R \Delta \mathbf{D} R^t)_{ij}$ , where  $\tilde{\epsilon}_{ij}$  is the unit strain tensor as before. The nonzero element of the unit strain tensor corresponding to the geometry of the experiment is the  $zz$  component. In matrix form, it is

$$\begin{bmatrix} 0 & 0 & 0 \\ 0 & 0 & 0 \\ 0 & 0 & 1 \end{bmatrix}. \quad (28)$$

The evaluation of  $\tilde{\epsilon}_{ij}(R\Delta DR^t)_{ij}$  gives  $\cos(2\psi)\sin^2(\theta)$  so that  $\gamma_z$  is related to the Euler angles  $\psi$ ,  $\theta$ ,  $\phi$  of the random rotations by

$$\gamma_z = \gamma_l \cos(2\psi) \sin^2(\theta). \quad (29)$$

This is the elastic equivalent of the  $d_z = d \cos(\theta)$  expression in the electric dipole case. Had the direction of the strain field been chosen to be along the  $x$  axis, the projection would have been

$$\begin{aligned} \tilde{\epsilon}_{ij}(R\Delta DR^t)_{ij} &= \cos(\theta) \sin(2\psi) \sin(2\psi) \\ &+ \cos(2\phi) \cos^2(\psi) \\ &- \cos^2(\psi) \cos(2\phi) \cos^2(\theta). \end{aligned} \quad (30)$$

Regardless of which expression is used, however, the results obtained below are the same, as they should be.

It is difficult to obtain an analytic form for the probability  $P(\gamma_z)$ . Instead, TLS with asymmetry  $\Delta$ , tunneling  $\Delta^o$  and  $\gamma_z$  as given by Eqs. (2) and (29) were generated numerically for the TLS model. For the modified TLS case,  $\Delta$  was sampled from a flat distribution, while  $\gamma_{l,t}$  and  $\gamma_z$  were generated using Eqs. (18) and (29).  $\Delta^o$  was obtained from  $\gamma_{l,t}$  using Eq. (20). In addition, an electric dipole moment projected along the direction of the qubit AC field,  $d_{||}$ , was generated from a flat distribution (up to 4 Debye) to compute the effective coupling to the qubit given by  $d_{||}\Delta^o/\epsilon$ . This effective coupling must have a minimal strength for the TLS to be visible. This minimal value was set to 0.01 Debye. Since  $\epsilon$  can vary between  $\hbar\omega_{q,\min}$  and  $\hbar\omega_{q,\max}$  along a spectroscopic trace,  $\epsilon$  is set to  $\hbar\omega_{q,\max}$  in the expression for the TLS-qubit coupling strength,  $d_{||}\Delta^o/\epsilon$ . Thus only TLS that are visible at the top of the spectroscopic window (for the appropriate applied strain field) are retained. The maximal value of  $\gamma_z$  for  $\text{SiO}_2$ ,  $\gamma_{z,\max}$ , is estimated to be 2.5 eV [8].  $\gamma_{z,\max}\alpha$  was chosen to be 0.5 GHz/Volt, which corresponds to a factor  $\alpha = 8 \times 10^{-7}$ .

In each case, it was determined whether the resulting TLS would cross into the spectroscopic window of the qubit. Crossing is defined as a TLS trace that covers at least 10% of the spectroscopic window along the frequency and/or voltage axis. This is done to account for the experimental need to see enough of the trace to obtain the fit necessary to extract  $\gamma_z\alpha$ . The calculations are very insensitive to this definition. The results are shown in Fig. 3: the top left plot shows the prediction of the standard TLS model, the top right plot is the prediction of the modified TLS model, and the lower plot corresponds to the measurements.

While the predictions of the standard and modified TLS models are quite distinct, neither come close to reproducing the measurements. A surprising feature of the experimental data is that the distribution is peaked at small values and decreases fairly quickly. The sharp decrease of the number TLS observed with large values of  $\gamma_z\alpha$  in the modified TLS model is due to the correlation between  $\Delta^o$  and  $\gamma_z$ . This decrease is, however, too sharp.

Then what can explain the peak at low  $\gamma_z\alpha$  and the tails in the distribution? A possible explanation involves the static fields. The assumption has hitherto been that they are uniform within the region where TLS can be measured. This may not

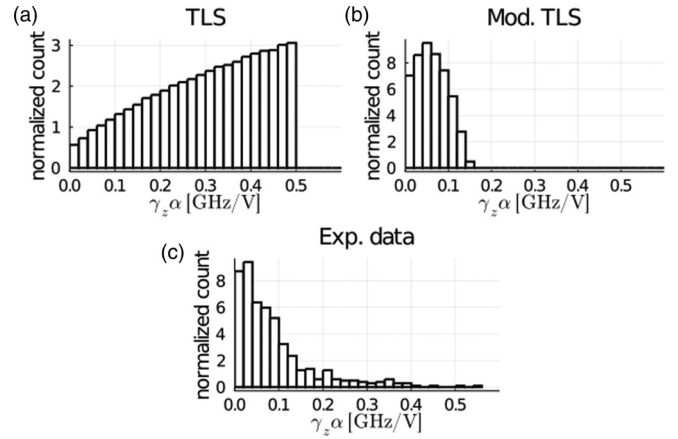


FIG. 3. Prediction for  $\gamma_z\alpha$  as measured in Ref. [12]. (a) TLS model prediction. (b) Modified TLS model. (c) Experimental data.

be the case, particularly in the elastic situation. What we may have is a gradient of the field, as exists inside a bent plate for instance (see Appendix B for an analysis of this situation) or regions where the field strengths may vary spatially. At long length scales, strain field have definite values as captured by elasticity theory. However, in the case of amorphous materials, the strain may vary substantially at the short distances characteristic of the assumed size of TLS [18]. To see the impact that such random variations may have on the observed distribution of  $\gamma_z\alpha$ ,  $\gamma_z\alpha$  was multiplied by Gaussian noise with mean 1 and standard deviation 0.5. The standard deviation was chosen to reproduce roughly the size of the peak in the distribution at low couplings. The result is shown in Fig. 4.

While there is no doubt that strain varies locally for a given applied external stress, is the scale of the fluctuation assumed here realistic? To answer this question, numerical simulations on amorphous  $\text{Al}_2\text{O}_3$  were performed. The system size is  $8.3 \text{ nm} \times 7.4 \text{ nm} \times 3.3 \text{ nm}$  ( $xyz$ ) and consists of 19 440 atoms. The distribution of strain inside the material was measured at  $T = 0 \text{ K}$  as a function of domain size ranging between 4 and 50 Å. The details of these simulations are

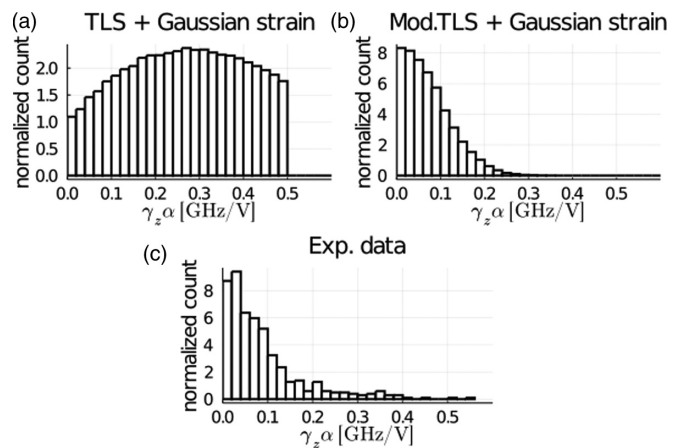


FIG. 4. Prediction for the distribution of  $\gamma_z\alpha_m$  using the TLS model and the modified TLS model, including intrinsic Gaussian strain fluctuations. (a) TLS model plus Gaussian strain fluctuations. (b) Modified TLS model plus Gaussian strain fluctuations. (c) Experimental data.



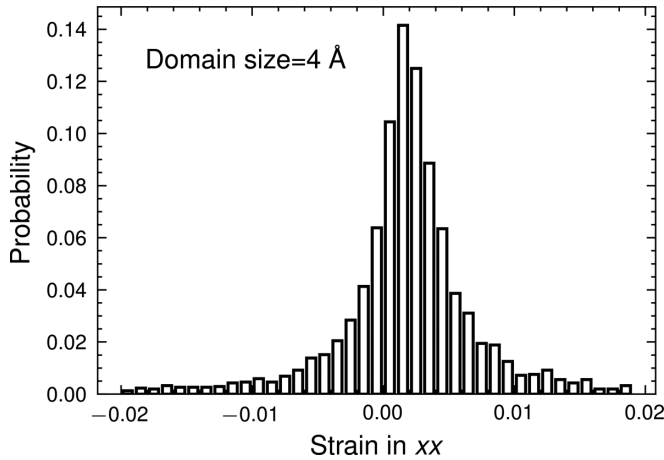


FIG. 5. Computed distribution of internal strains for an external strain  $\epsilon_{xx}^{\text{ext}} = 2 \times 10^{-3}$ . Domain size is 4 Å.

given in Appendix A. A given overall dilatation was applied along the  $x$  axis,  $\epsilon_{xx}^{\text{ext}} = 2 \times 10^{-3}$ , of the numerical sample. This value is large compared to the strains actually applied to the qubits ( $\sim 10^{-6}$ ) but are still within the elastic regime. An example of the distribution of internal strains is shown in Fig. 5. The distribution for shear strains,  $\epsilon_{xy}^{\text{ext}} = 2 \times 10^{-3}$ , shows a very similar behavior, albeit with a larger variance. As the size of the domain increases, the distribution becomes increasingly peaked around a mean value equal to the externally applied strain. Figure 6 shows the reduction in variance as a function of domain size.

The variance for a domain size comparable to the size of a TLS, i.e.,  $\sim 20$  Å, is about  $10^{-6}$  which, when normalized by the externally applied strain so as to be applicable to the experimental strains, corresponds to a standard deviation of 0.5 as was used earlier. Note that the distribution of internal strains has larger tails than a normal distribution. This may very well explain the long tail in the experimental distribution of couplings (see Fig. 4). The conclusion of this analysis is that the strain variations observed in simulations of amorphous alumina are compatible with the variations required

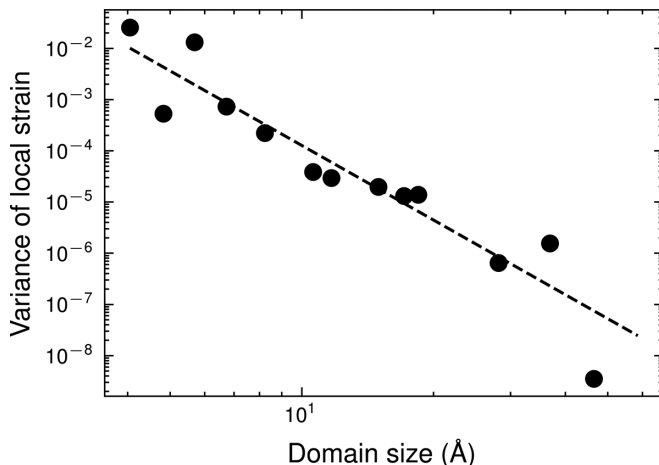


FIG. 6. Evolution of the internal strain variance as a function of domain size (in Å). The external strain is  $\epsilon_{xx}^{\text{ext}} = 2 \times 10^{-3}$ .

to account for the observed distribution of couplings  $\gamma_z \alpha$  in qubits.

It is of course possible that the distribution of TLS in the thin amorphous layers where they can be observed is simply far from the bulk values which were assumed to hold. For instance, consider TLS with large asymmetry energies that lie well above the observation window and can only be pulled into that window if they have a large TLS-phonon coupling. If the distribution of  $\Delta$  decreases with increasing asymmetry energies, the number of TLS that are observed with large TLS-phonon couplings would decrease accordingly. The TLS may also reside in greater numbers at the interfaces between the amorphous layers and its surroundings (vacuum, conducting plates, etc.). These TLS may have distributions that are quite different from their bulk counterparts. The interface also creates a preferential direction that may substantially affect the orientation of the dipole moments.

#### IV. CONCLUSION

This work addresses the question as to whether the strength of electric dipole moments and elastic dipole moments associated with two level systems in glasses are distributed over a wide range of values as in the modified TLS model or are narrowly centered around a given value as in the standard TLS model. The dielectric and elastic data favor the first possibility. The situation in the elastic case requires that local random strain fluctuations be included and the distribution of these random strains are consistent with those found from molecular dynamics simulations. However, we note the fairly good agreement between experiments and the modified TLS model is not so much due to the distribution of couplings as it is to the correlation between the tunneling matrix element and the elastic coupling strength. While that correlation implies a wide range of couplings, the distribution itself is not the key element leading to the results. This is in part due to the fact that even with a single value for the magnitude of the field-TLS coupling assumed by the standard TLS model, a range of values for the projection along the applied field is nevertheless present due to the random orientation of the dipoles. The good agreement between the modified TLS model and the experimental observations suggests a significant correlation between the tunneling matrix element  $\Delta^o$  and the elastic TLS phonon coupling.

#### ACKNOWLEDGMENTS

H.M.C., Z.Y., B.W., Z.W., J.R.S., and C.C.Y. were supported by the National Science Foundation (NSF) through the University of Wisconsin Materials Research Science and Engineering Center (NSF Grant No. DMR-1720415). A.B. and J.L. acknowledge funding from Google LLC. J.L. is grateful for funding from the Baden-Württemberg-Stiftung.

#### APPENDIX A: SIMULATIONS ON AMORPHOUS $\text{Al}_2\text{O}_3$

The molecular dynamics simulations in this study were conducted with the LAMMPS package [19] using empirical potentials developed for aluminosilicate melts by Matsui [20].

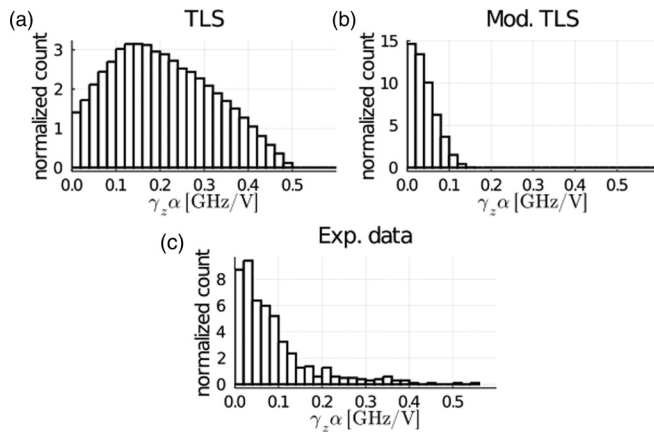


FIG. 7. Prediction for the distribution of  $\gamma_z \alpha_m$  using the TLS model and the modified TLS model, including an intrinsic strain gradient. (a) TLS model. (b) Modified TLS model. (c) Experimental data.

The amorphous alumina structures produced by the potentials were found to be in good agreement with experimental observations. The system used for the strain calculations was a bulk  $\text{Al}_2\text{O}_3$  structure with periodic boundary conditions containing 19 440 atoms in total. To prepare the amorphous structure, the system was first melted at 5000 K for 100 ps and then quenched to 100 K using a cooling rate of 1 K/ps, in the isothermal-isobaric ensemble (NPT). Based on the enthalpy-temperature cooling curve, the glass transition occurred around 1300 K. The melt-quench procedure resulted in an amorphous system with the size of  $8.3 \text{ nm} \times 7.4 \text{ nm} \times 3.3 \text{ nm}$  at 100 K. Subsequently, the system was relaxed to 0 K for the strain calculations. The relaxed structure was subjected to uniaxial strains of  $-0.004$ ,  $-0.002$ ,  $0$ ,  $0.002$ , and

$0.004$ . At each strain, the structure is relaxed in the canonical ensemble (NVT) before the strains are analyzed. The resulting strain-stress curve for the whole system was linear, suggesting that the system stayed within the elastic region.

To investigate the local strain distribution, the system was relaxed under a given external strain and divided into small cuboid boxes. The local strain in each box was then calculated by averaging the vectorial transformation from every atom in the box to a reference atom. By changing the cuboid box size, local strain distributions at different length scales were obtained. Note that the geometric average of the three sizes of the cuboid box needed to be greater than 0.4 nm to ensure that at least two atoms are in each box.

## APPENDIX B: EFFECT OF UNIFORM STRAIN GRADIENTS

A linear gradient of the strain field in the regions where the TLS are located will also affect the observed distribution of  $\gamma_z \alpha$ . To assess the impact of such a gradient, a simulation with a linear strain gradient was performed. The variation in  $\alpha V_p$  was taken to be linear, decreasing from the maximal value to 0.25 of that maximal value for a given piezo voltage. The maximal value is determined by the coefficient  $\alpha = 8 \times 10^{-7}$  as before. The results are shown in Fig. 7.

While the effect of the linear strain gradient improves the results somewhat, the effect is marginal. The experimental observation that surface TLS and junction TLS show essentially the same distribution while one would expect the junction TLS to experience a much more uniform strain, lends support to the idea that strain gradients do not play an important role.

- [1] P. W. Anderson, B. I. Halperin, and C. M. Varma, Anomalous low-temperature thermal properties of glasses and spin glasses, *Philos. Mag.* **25**, 1 (1972).
- [2] W. A. Phillips, Tunneling states in amorphous solids, *J. Low Temp. Phys.* **7**, 351 (1972).
- [3] W. A. Phillips, Two-level states in glasses, *Rep. Prog. Phys.* **50**, 1657 (1987).
- [4] S. Hunklinger and A. Raychaudhuri, Chapter 3: Thermal and elastic anomalies in glasses at low temperatures, in *Progress in Low Temperature Physics*, Vol. 9 (Elsevier, 1986), pp. 265–344.
- [5] J. J. Freeman and A. C. Anderson, Thermal conductivity of amorphous solids, *Phys. Rev. B* **34**, 5684 (1986).
- [6] K. Topp and D. G. Cahill, Elastic properties of several amorphous solids and disordered crystals below 100 k, *Z. Phys. B* **101**, 235 (1996).
- [7] J. F. Berret and M. Meißner, How universal are the low temperature acoustic properties of glasses?, *Z. Phys. B* **70**, 65 (1988).
- [8] H. M. Carruzzo and C. C. Yu, Why Phonon Scattering in Glasses is Universally Small at Low Temperatures, *Phys. Rev. Lett.* **124**, 075902 (2020).
- [9] J. Joffrin and A. Levelut, Virtual phonon exchange in glasses, *J. Phys.* **36**, 811 (1975).
- [10] K. Kassner and R. Silbey, Interactions of two-level systems in glasses, *J. Phys.: Condens. Matter* **1**, 4599 (1989).
- [11] C. Müller, J. H. Cole, and J. Lisenfeld, Towards understanding two-level-systems in amorphous solids: Insights from quantum circuits, *Rep. Prog. Phys.* **82**, 124501 (2019).
- [12] G. J. Grabovskij, T. Peichl, J. Lisenfeld, G. Weiss, and A. V. Ustinov, Strain tuning of individual atomic tunneling systems detected by a superconducting qubit, *Science* **338**, 232 (2012).
- [13] J. Lisenfeld, A. Bilmes, S. Matityahu, S. Zanker, M. Marthaler, M. Schechter, G. Schön, A. Shnirman, G. Weiss, and A. V. Ustinov, Decoherence spectroscopy with individual two-level tunneling defects, *Sci. Rep.* **6**, 23786 (2016).
- [14] D. A. Parshin, H. R. Schober, and V. L. Gurevich, Vibrational instability, two-level systems, and the boson peak in glasses, *Phys. Rev. B* **76**, 064206 (2007).
- [15] B. Sarabi, A. N. Ramanayaka, A. L. Burin, F. C. Wellstood, and K. D. Osborn, Projected Dipole Moments of Individual Two-Level Defects Extracted using Circuit Quantum Electrodynamics, *Phys. Rev. Lett.* **116**, 167002 (2016).
- [16] J. M. Martinis, K. B. Cooper, R. McDermott, M. Steffen, M. Ansmann, K. D. Osborn, K. Cicak, S. Oh, D. P. Pappas, R. W.

- Simmonds, and C. C. Yu, Decoherence in Josephson Qubits from Dielectric Loss, *Phys. Rev. Lett.* **95**, 210503 (2005).
- [17] J. Lisenfeld, A. Bilmes, A. Megrant, R. Barends, J. Kelly, P. Klimov, G. Weiss, J. M. Martinis, and A. V. Ustinov, Electric field spectroscopy of material defects in transmon qubits, *npj Quantum Inf.* **5**, 105 (2019).
- [18] A. J. G. Lunt, P. Chater, and A. M. Korsunsky, On the origins of strain inhomogeneity in amorphous materials, *Sci. Rep.* **8**, 1574 (2018).
- [19] S. Plimpton, Fast parallel algorithms for short-range molecular dynamics, *J. Comput. Phys.* **117**, 1 (1995).
- [20] M. Matsui, A transferable interatomic potential model for crystals and melts in the system cao-mgo-al2o3-sio2, *Mineral. Mag.* **58A**, 571 (1994).